ELSEVIER

Journal of Wind Engineering
and Industrial Aerodynamics 67 & 68 (1997) 493–506

JOURNAL OF wind engineering AND industrial aerodynamics

A numerical study of stably stratified flows over a two-dimensional hill – Part I. Free-slip condition on the ground

T. Uchida[a,*], Y. Ohya[b]

[a] *Interdisciplinary Graduate School of Engineering Sciences, Kyushu University, Kasuga 816, Japan*
[b] *Research Institute for Applied Mechanics, Kyushu University, Kasuga 816, Japan*

Abstract

Stably stratified flows over a two-dimensional hill in a channel of finite depth are analyzed numerically by using a newly-developed multi-directional finite-difference method at a Reynolds number Re = 2000. To simplify the phenomena occurring in the flow around the hill, the free-slip condition for the velocity is assumed on the ground, and the nonslip condition is imposed only on the hill surface. Attention is focused on the unsteadiness in the flow around the hill for the cases of $K(=NH/\pi U)>1$ where N and U are the buoyancy frequency and free-stream velocity and H is the domain depth. The flow unsteadiness is discussed, being associated with shedding of the upstream advancing columnar disturbance.

Keywords: Direct numerical simulation; Finite-difference method; Stably stratified flow; Two-dimensional hill

1. Introduction

In the atmospheric boundary layer, buoyancy force associated with density stratification plays a key role. It damps or enhances vertical motion directly in the stratified flows. When a stably stratified fluid flows over topography, vertically disturbed air parcels can lead to generation of downstream lee waves, which cause drastic changes in the flow pattern.

It is well known from laboratory experiments (see, e.g. Refs. [1,2]) that, in the linearly stratified flow of finite depth, columnar disturbances, which have discrete vertical modes, propagating upstream of an obstacle always appear when lee

* Corresponding author.

PII S0167-6105(97)00096-2

waves exist. The columnar disturbance is a manifestation of the long internal wave which causes an almost horizontal motion relative to the basic flow. According to the linear theory, for stratified fluid of finite depth H, the flow is characterized by the parameter $K\,(=NH/\pi U)$ where N and U are the buoyancy frequency and free-stream velocity. For weak stratification (i.e. $K \leqslant 1.0$), all modes have velocities less than free-stream velocity and are swept downstream with no lee waves, while for strong stratification (i.e. $K > 1.0$), stationary lee waves can form and columnar modes propagate upstream.

For stably stratified flows over a two-dimensional obstacle in a channel of finite depth, there are many findings from both experiments [1,2] and numerical simulations [3–7]. The most striking feature of those findings is the unsteadiness of the flow around an obstacle for strong stratification. Castro et al. [2] found in their experiments that the obstacle drag in linearly stratified flows shows a persistent periodical oscillation under a certain stratification. Similar phenomena have been confirmed in some numerical calculations under similar situations [4–7]. As to the mechanism of the flow unsteadiness, various discussions have been given [4–7], however, it still remains unclear.

The numerical simulations reported above have been made at low Reynolds numbers only as high as $\mathrm{Re} = 100$. Therefore, it is difficult to compare those results with experimental ones ($\mathrm{Re} = 10^3$–10^4) directly. We have tried to clarify the effect of stable stratification on unsteady, separated and reattaching flows behind an obstacle at higher Reynolds numbers both experimentally [8] and numerically [8,9]. In general, for higher Re, the flow over an obstacle becomes more complex owing to the unsteady separated and reattaching flow behind the obstacle. In the present numerical study, we have investigated the linearly stratified flows over a two-dimensional hill at $\mathrm{Re} = 2000$ by using a newly-developed multi-directional finite-difference method. Particular emphasis is given to the mechanism of flow unsteadiness around a hill for strong stratification (i.e. $K > 1.0$). Therefore, to simplify the phenomena occurring in the flow around a hill, the free-slip condition for the velocity is assumed on the ground, and the nonslip condition is imposed only on the hill surface.

2. Numerical model

2.1. Physical domain and computational grid

We consider a linearly stratified flow of incompressible and nondiffusive fluid past a two-dimensional hill in a channel of finite depth. A typical physical domain is shown in Fig. 1. The inflow boundary is set sufficiently far away to delay the arrival of upstream reflection ($x = -420h$ for all cases). A cosine function is chosen for the geometry of the hill with its profile given by $h(x) = 0.5\{1 + \cos(\pi x/a)\}$, where the width parameter a is set equal to 1. In order to simulate the flow around the hill with high accuracy, a body-fitted coordinate system is employed. The number of grid points in the x- and z-directions are 421×101 for all cases. Moreover, we have studied

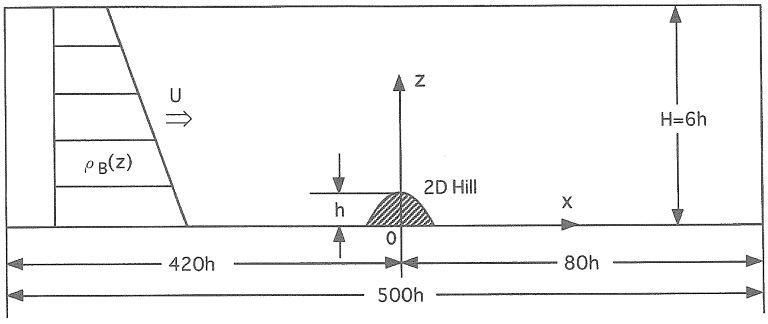

Fig. 1. Physical domain.

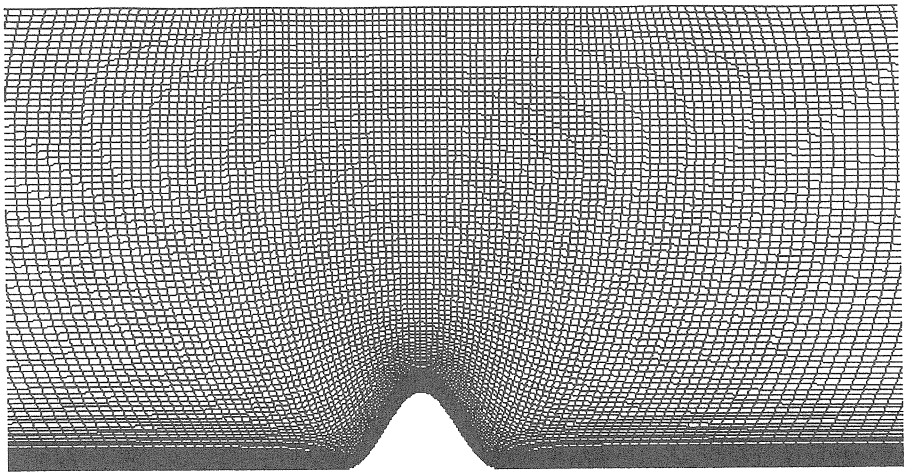

Fig. 2. Computational grid near the hill.

the other two grid systems which have 351×51 and 421×76 points, respectively. The changes in the grid resolution were found to have negligible effect on the numerical results, therefore, we expect that the present calculations are free from grid dependence. The computational grid near the hill is shown in Fig. 2. The grid points in the physical domain are concentrated toward the hill surface and the ground. The vertical smallest grid spacing is $3.0 \times 10^{-3}h$ at the hill top.

2.2. Governing equations

Under the Boussinesq approximations, the dimensional governing equations consist of the continuity equation, the Navier–Stokes equations, and the density equation

as follows,

$$\frac{\partial u_i}{\partial x_i} = 0, \tag{1}$$

$$\frac{\partial u_i}{\partial t} + u_j \frac{\partial u_i}{\partial x_j} = -\frac{1}{\rho_0}\frac{\partial p'}{\partial x_i} + \frac{\mu}{\rho_0}\frac{\partial^2 u_i}{\partial x_j \partial x_j} - \frac{\rho' g \delta_{i3}}{\rho_0}, \tag{2}$$

$$\frac{\partial \rho'}{\partial t} + u_j \frac{\partial \rho'}{\partial x_j} = -w\frac{\mathrm{d}\rho_B}{\mathrm{d}z}, \tag{3}$$

ρ', p' are the perturbation density and pressure defined as

$$\rho = \rho_B(z) + \rho', \qquad p = p_B(z) + p', \tag{4}$$

where $\rho_B(z)$ and $p_B(z)$ are the undisturbed distributions at the inflow boundary, and $\rho_B(z)$ decreases upward linearly, $u_i = (u, w)$ is the velocity, ρ_0 is the reference density, g is the acceleration due to gravity, and μ is the viscosity coefficient.

Nondimensionalizing the variables using the free-stream velocity U, the hill height h, and the reference density ρ_0, we have three dimensionless equations as follows:

$$\frac{\partial u_i}{\partial x_i} = 0, \tag{5}$$

$$\frac{\partial u_i}{\partial t} + u_j \frac{\partial u_i}{\partial x_j} = -\frac{\partial p}{\partial x_i} + \frac{1}{\mathrm{Re}}\frac{\partial^2 u_i}{\partial x_j \partial x_j} - \frac{\rho}{\mathrm{Fr}^2}\delta_{i3}, \tag{6}$$

$$\frac{\partial \rho}{\partial t} + u_j \frac{\partial \rho}{\partial x_j} = w. \tag{7}$$

These equations include two dimensionless parameters, i.e., the Reynolds number Re ($= \rho_0 Uh/\mu$) and the Froude number Fr ($= U/Nh$), where N is the buoyancy frequency defined as $N^2 = -(g/\rho_0)(\mathrm{d}\rho/\mathrm{d}z)$. It should be noted that for the finite depth flow not only Re and Fr but also K ($= NH/\pi U$), which contains the domain depth H, is a parameter necessary to determine the character of the internal gravity wave. Since K is rewritten as $K = H/\pi h\mathrm{Fr}$, it is determined by H/h when Fr is a known number. In other words, K reflects the effect of boundary conditions though it does not appear explicitly in the governing equations. We use the parameter K as a stability parameter in this study.

2.3. *Finite-difference method*

Through a coordinate transformation ($x = x(\xi, \zeta)$, $z = z(\xi, \zeta)$), the governing equations (Eqs. (5)–(7)) are solved in the computational domain using a finite-difference

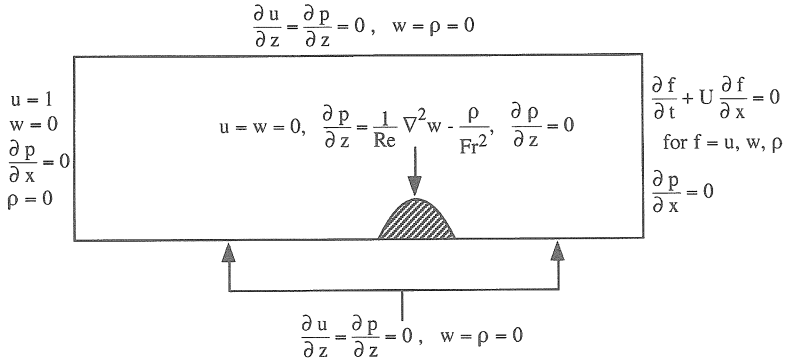

Fig. 3. Boundary conditions.

method. The numerical method used is an extension of the MAC method to the incompressible stratified flow, and the Poisson equation for pressure derived by taking divergence of Eq. (6) is solved by the SOR method. The regular grid arrangement for variables is employed. The Euler explicit method with first-order accuracy is used for time advance in Eqs. (6) and (7). All of the spatial derivatives except for the convective terms are approximated by a second-order central scheme. For the convective terms, a third-order upwind scheme is employed to minimize the numerical dissipation of velocities and density. Moreover, for all the spatial derivatives, a newly-developed multi-directional finite-difference method [10], which leads to a calculation of much higher accuracy, is used.

The boundary conditions are shown in Fig. 3. The condition $\partial u/\partial z = 0$ on the upper boundary and the ground except for the hill in Fig. 3 is the free-slip condition. In general, understanding the evolving flow field is complicated by a number of factors, particularly in boundary layer phenomena. To avoid such a troublesome boundary layer effect, which usually appears in laboratory experiments, we chose the free-slip condition on the ground both upstream and downstream ($|x| > a$) of the hill. The nonslip condition is imposed only on the hill surface ($|x| \leqslant a$). Impulsive-start ($u = 1, w = 0, p = 0, \rho = 0$) is employed for an initial condition. We calculate the flows at a Reynolds number $\mathrm{Re} = 2000$ for a wide range of K ($0 \leqslant K \leqslant 3.0$). The nondimensional time step is 2×10^{-3}.

3. Results and discussions

3.1. Weak stratification ($0 \leqslant K \leqslant 1.0$)

Fig. 4 shows the instantaneous streamlines around the hill for weak stratification cases of $0 \leqslant K \leqslant 1.0$ at a nondimensional time $t = 200$. A stationary vortex behind the hill is observed and its length is shortened as K increases. It should be noted that for the cases of $K = 0$–0.8, a stationary vortex becomes longer gradually as time

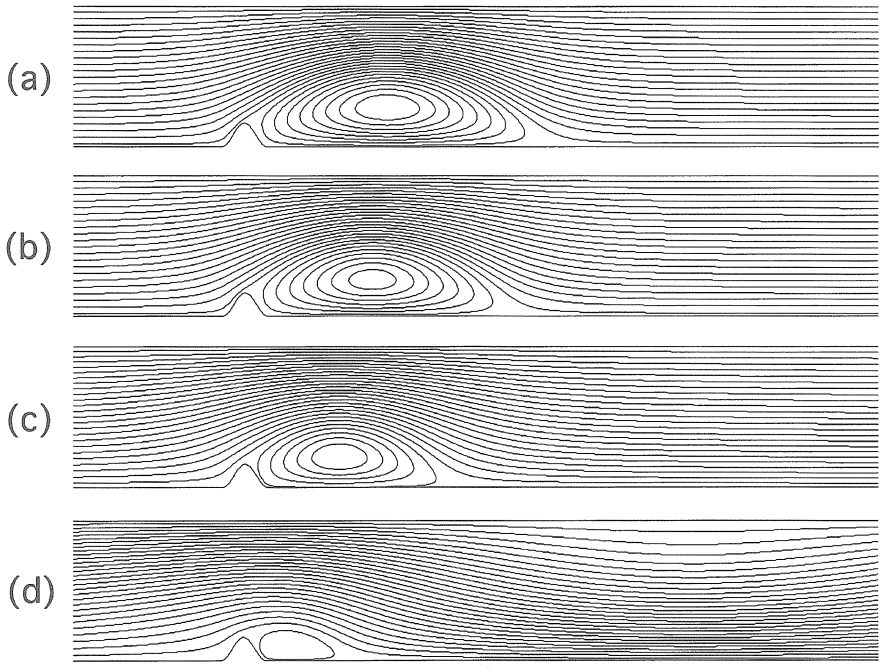

Fig. 4. Instantaneous streamlines at a nondimensional time $t = 200$, Re = 2000: (a) $K = 0$, (b) $K = 0.5$, (c) $K = 0.8$, (d) $K = 1.0$.

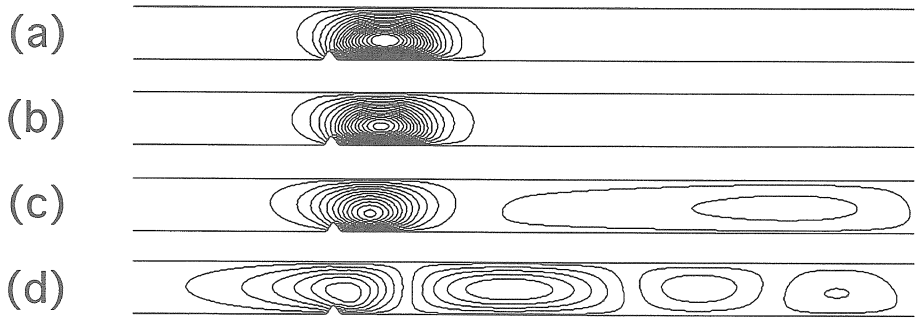

Fig. 5. Perturbation streamlines $\Delta\psi$ $(-4 \leqslant \Delta\psi \leqslant 2)$ at $t = 200$, Re = 2000: (a) $K = 0$, (b) $K = 0.5$, (c) $K = 0.8$, (d) $K = 1.0$.

proceeds. For $K \geqslant 0.8$, stationary lee waves with long wavelength appear (these can be observed more clearly in Fig. 5c and Fig. 5d), but for the case of $K = 0.8$, this lee wave disappears at $t = 500$. Thus, the stratification acts largely to modify the separated wake due to the generation of lee waves.

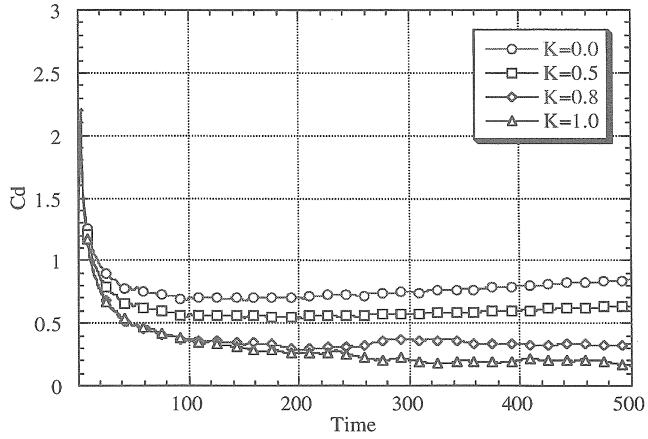

Fig. 6. Time development of drag coefficient C_d for the cases of $0 \leqslant K \leqslant 1.0$, Re = 2000.

Fig. 5 shows the perturbation streamlines ($\Delta\psi$), which are depicted by the perturbation velocities u' and w', i.e. $u' = U - u$, $w' = w$, at $t = 200$. These perturbation streamlines make clear the existence of lee waves and columnar disturbances propagating upstream of the hill. In Fig. 5c and Fig. 5d, closed perturbation streamlines, which mean the existence of lee waves, are observed in the downstream of the hill. In Fig. 5a–5d, systematic upstream propagations of columnar disturbances are not yet observed, although extended upstream disturbances are observed for the case of $K = 1.0$ in Fig. 5d.

Time development of drag coefficient C_d over a period of integration $0 \leqslant t \leqslant 500$ is shown in Fig. 6. The behavior of C_d for all cases suggests that the flow around the hill for weak stratification cases of $0 \leqslant K \leqslant 1.0$ reaches an almost steady condition. But exactly speaking, these C_d values never reach a constant value, reflecting gradual elongation of the size of the stationary vortices.

The stable stratification effects on the flow over a hill for weak stratification cases of $0 \leqslant K \leqslant 1.0$ at a Reynolds number of 2000 are almost similar to those at low Reynolds numbers ($Re \leqslant 100$) of Castro [3], Hanazaki [4,5] and Paisley et al. [7].

3.2. *Strong stratification ($1.0 < K \leqslant 3.0$)*

Fig. 7 shows the instantaneous streamlines around the hill for strong stratification cases of $1.0 < K \leqslant 3.0$. The lee wavelength is gradually shortened as K increases. The first upward flow in the lee wave motion induces a rotor (secondary separation) on the downstream ground. We can see another rotor on the upper boundary, the location of which gradually approaches $x = 0$ as the lee wavelength is shortened, as seen in Fig. 7a–7d. These rotors seem to behave as a downstream obstacle. Moreover, for the cases of $K = 2.5$ and 3.0 in Fig. 7e and Fig. 7f, "lee wave-breaking" can be observed.

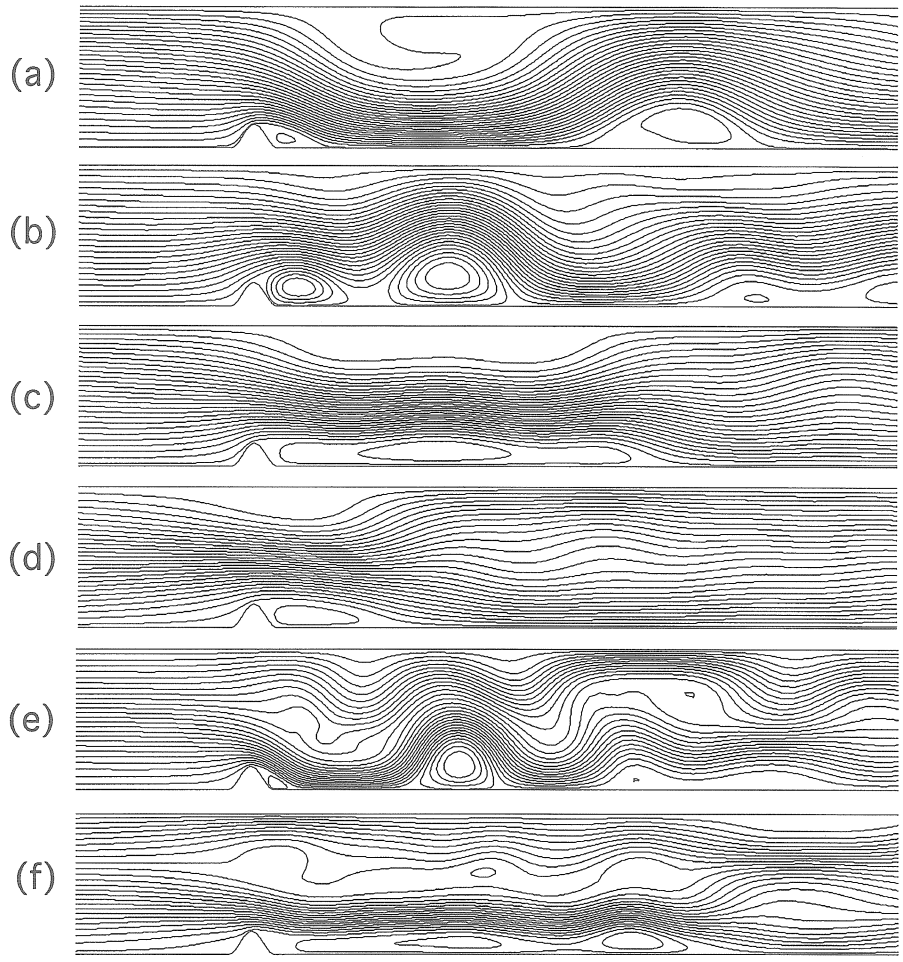

Fig. 7. Instantaneous streamlines at $t = 200$, Re $= 2000$: (a) $K = 1.25$, (b) $K = 1.5$, (c) $K = 1.75$, (d) $K = 2.0$, (e) $K = 2.5$, (f) $K = 3.0$.

Fig. 8 shows the perturbation streamlines ($\Delta\psi$). The wave of mode $n = 1$ begins to propagate upstream in the form of a columnar disturbance. The "detaching" of the eddy is seen since the strong and weak part appear, in turn, in each mode of upstream advancing columnar disturbances. As K becomes larger, the mode $n = 1$ eddy is detached successively at a shorter period. When $K \geqslant 1.75$ in Fig. 8c–8e, the columnar disturbances with mode $n = 2$ also propagate upstream of the hill and when $K = 3.0$ in Fig. 8f, those with mode $n = 3$ are seen clearly. It should be noted that the columnar disturbances with mode $n = 1$ generated as "detaching eddies" have only the clockwise circulation for the case of $K = 1.25$, while for the cases of $K \geqslant 1.5$, they have both clockwise and counter-clockwise circulations. A detaching eddy (columnar

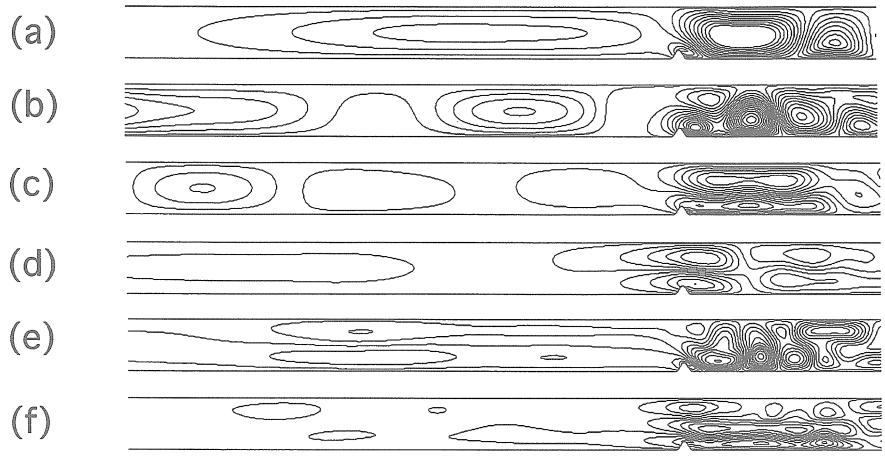

Fig. 8. Perturbation streamlines $\Delta\psi$ ($-4 \leqslant \Delta\psi \leqslant 2$) at $t = 200$, Re = 2000: (a) $K = 1.25$, (b) $K = 1.5$, (c) $K = 1.75$, (d) $K = 2.0$, (e) $K = 2.5$, (f) $K = 3.0$.

disturbance) with clockwise circulation is generated from below around the hill, on the other hand, the one with counter-clockwise circulation is generated from the above near the upper boundary. The origin of the detaching eddy (columnar disturbance) from the above seems to be a rotor on the upper boundary when it is generated very close to $x = 0$ by a short lee wavelength.

According to the linear theory, the propagation speed of the columnar disturbance (eddy) with mode $n = 1$ is given by $(K - 1)U$. The value obtained by the present calculation is consistent with the prediction of the linear theory for the cases of $K \geqslant 1.25$.

Fig. 9 shows the time development of C_d for the cases of $1.25 \leqslant K \leqslant 2.0$ over a period of integration $0 \leqslant t \leqslant 500$. The most striking feature in Fig. 9 is the persistent periodical C_d oscillations for the cases of $K = 1.25$ and 1.5, while for the cases of $K = 1.75$ and 2.0, these oscillations rapidly decay after $t = 200$. These C_d oscillations suggest that the flow around the hill under strong stratification is intrinsically unsteady. Especially for the case of $K = 1.5$, the amplitude of C_d oscillations is very large. These features of C_d variations in time for the cases of $K = 1.25$–2.0 are very similar to the results of Paisley et al. [7]. We will discuss a possible mechanism of the flow unsteadiness in more detail in the next section.

3.3. *Discussions of the flow unsteadiness ($1.0 < K \leqslant 2.0$)*

Hanazaki [4,5] asserted that the C_d oscillations were the result of the columnar disturbance (eddy) detaching from the obstacle. Castro et al. [2] suggested that the C_d oscillations were driven by the changes in the effective value of K upstream of the obstacle as a consequence of the changes in the strength of the columnar disturbances. Lamb [6] stated that no upstream columnar disturbances which permanently modify

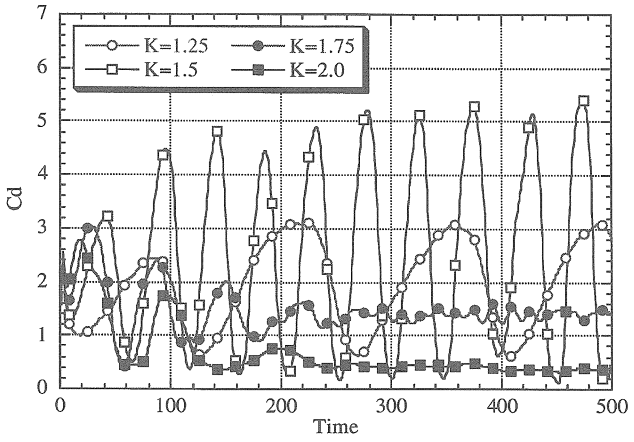

Fig. 9. Time development of C_d for the cases of $1.25 \leqslant K \leqslant 2.0$, Re = 2000.

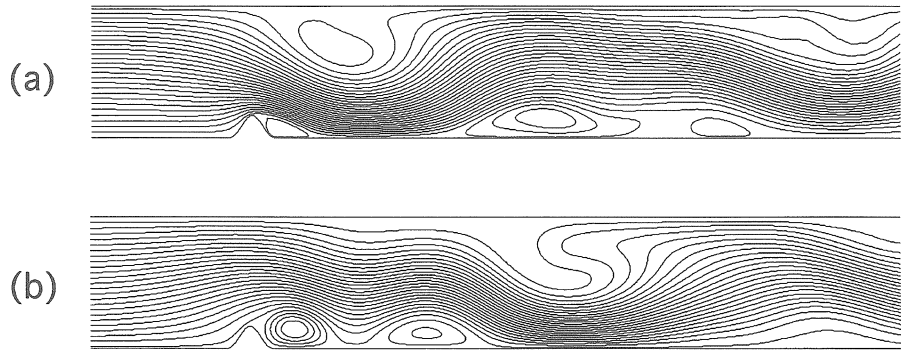

Fig. 10. Instantaneous streamlines for the case of $K = 1.5$, Re = 2000: (a) high-C_d state ($t = 425$), (b) low-C_d state ($t = 450$).

the upstream flow conditions were observed even though the C_d oscillations were seen. Paisley et al. [7] suggested that the unsteady behavior was the result of nonlinear processes.

We consider the flow unsteadiness for the cases of $1.25 \leqslant K \leqslant 2.0$ as follows. Fig. 10a and Fig. 10b show the instantaneous streamlines at high- and low-C_d states, respectively, for the case of $K = 1.5$. There is a large difference in the flow pattern between the two states. In a high-C_d state, we can see large-amplitude lee waves over the hill, while in a low-C_d state, these are small. Correspondingly, a small recirculating eddy behind the hill is induced in a high-C_d state, while a large one in a low-C_d state. Fig. 11a and Fig. 11b show the $\Delta\psi$ patterns corresponding to high- and low-C_d states, respectively. We should note that the columnar disturbance (eddy) with mode $n = 1$

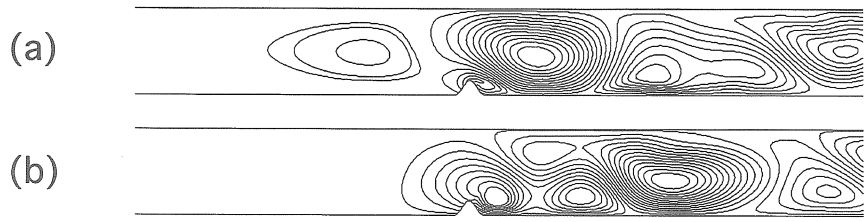

Fig. 11. Perturbation streamlines $\Delta\psi$ ($-4 \leqslant \Delta\psi \leqslant 2$) for the case of $K = 1.5$, Re $= 2000$: (a) high-C_d state ($t = 425$), (b) low-C_d state ($t = 450$).

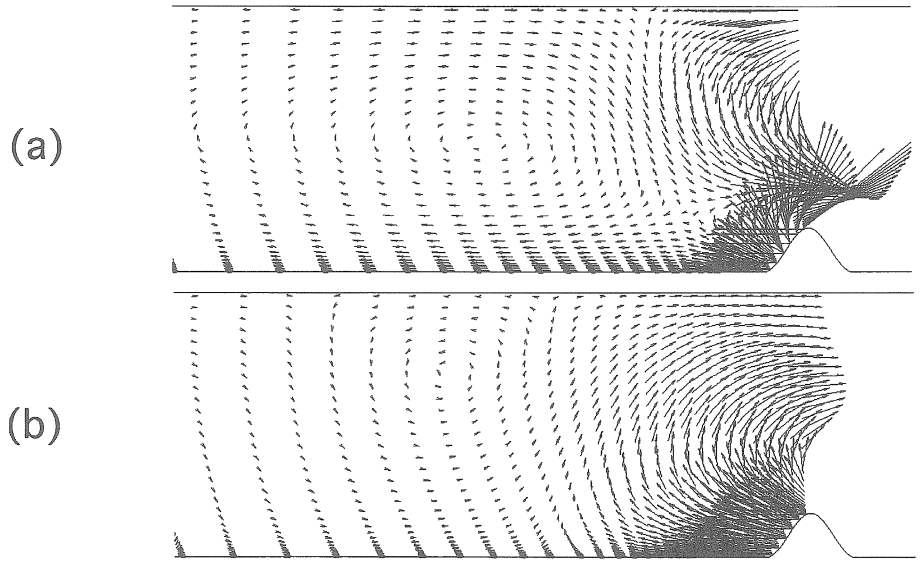

Fig. 12. Perturbation velocity vectors for the case of $K = 1.5$, Re $= 2000$: (a) high-C_d state ($t = 425$), (b) low-C_d state ($t = 450$).

has just detached from the hill in a high-C_d state, while the one is just about to detach from the hill in a low-C_d state. To examine the perturbation-flow field in more detail, the corresponding perturbation-velocity vectors near the hill are displayed in Fig. 12a and Fig. 12b. First, it can be observed that the columnar disturbance (eddy) with mode $n = 1$ has a clockwise circulation. Therefore, when the columnar disturbance (eddy) has just detached from the hill, it induces a downward flow in front of the hill as seen in Fig. 12a, on the other hand, when the columnar disturbance (eddy) is just about to detach from the hill, it induces an upward flow in front of the hill as seen in Fig. 12b. These downward and upward flows generated by the columnar disturbance (eddy) affect the approaching flow directly; the former tends to press down the approaching flow and the latter tends to lift it up. As a result, the curvature of the

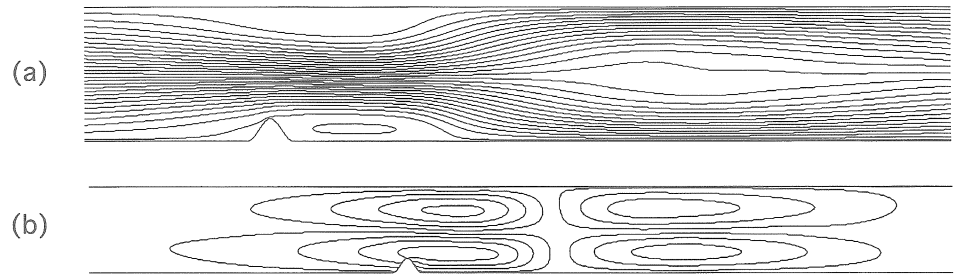

Fig. 13. Flow around the hill reached a steady condition for the case of $K = 2.0$ at $t = 500$, Re $= 2000$: (a) instantaneous streamlines, (b) perturbations streamlines $\Delta\psi$ ($-4 \leqslant \Delta\psi \leqslant 2$).

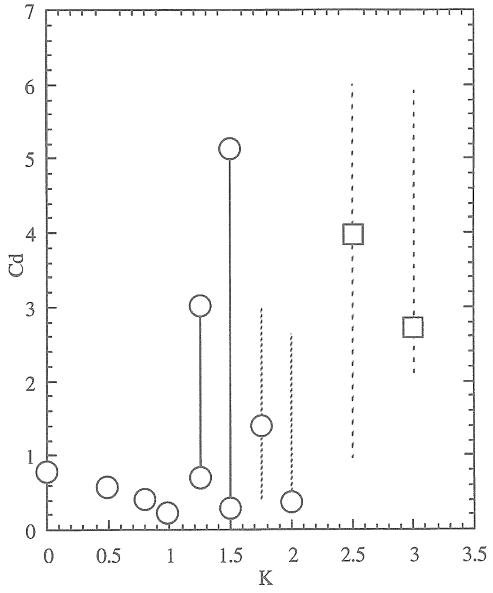

Fig. 14. Variations of C_d with K, Re $= 2000$. Full and dotted lines indicate persistent and decaying C_d oscillations, respectively. The behavior of C_d for $K = 2.5$ and 3.0 are still unclear.

separated and reattaching shear layer behind the hill becomes large as seen in Fig. 10a, while it becomes small as seen in Fig. 10b. Since the base pressure of the hill can be directly influenced by the curvature of the separated and reattaching shear layer, C_d becomes a high value due to the large curvature and a low value due to the small curvature. Thus, the alternating states of high- and low-C_d are caused by the shedding of the columnar disturbance (eddy) in the upstream of the hill. Accordingly, the period of C_d oscillations in Fig. 9 is consistent with that of the shedding of the columnar disturbances.

Next, we consider the reason of the decay of C_d oscillations for the cases of $K = 1.75$ and 2.0. For these cases, the columnar disturbance with mode $n = 2$ becomes dominant, for example, as shown in Fig. 13a and Fig. 13b for the case of $K = 2.0$. This leads to the flow around the hill to be a symmetric one with the horizontal center axis of finite domain. Therefore, as time proceeds, the flow around the hill tends to reach a steady condition for the cases of $K = 1.75$ and 2.0.

3.4. *Variation of C_d with $K(0 \leqslant K \leqslant 3.0)$*

Fig. 14 shows the variation of C_d with K for the cases of $0 \leqslant K \leqslant 3.0$. We can see that C_d decreases locally at integral values of $K = 1.0$, 2.0 and 3.0. The overall trend of C_d is similar to the previous numerical studies [4, 5, 7–9].

4. Conclusions

We have performed numerical calculations on the stratified flows over a two-dimensional hill in a channel of finite depth at $\mathrm{Re} = 2000$ for a wide range of K ($0 \leqslant K \leqslant 3.0$). To simplify the phenomenon occurring in the flow around the hill, the free-slip condition for the velocity is assumed on the ground, and the nonslip condition is imposed only on the hill surface. The major conclusions of the present study can be summarized as follows:

(1) As K increases, the recirculating eddy behind the hill is suppressed and its length is shortened. For the cases of $K \geqslant 0.8$, lee waves appear and affect strongly the flow behind the hill. The lee wavelength is shortened as K increases. For the cases of $K \geqslant 1.25$, the lee wave motion induces a rotor (secondary separation) on the downstream ground and another rotor on the upper boundary.

(2) From the perturbation streamlines ($\Delta\psi$), which are depicted by the perturbation velocities, the upstream advancing columnar disturbances (eddy) with mode $n = 1$ are observed when lee waves exist. When $K \geqslant 1.75$, the columnar disturbances with mode $n = 2$ also propagate upstream of the hill and when $K = 3.0$, those with mode $n = 3$ are seen clearly. The propagation speeds obtained by the present calculations are consistent with the prediction of the linear theory for the cases of $K \geqslant 1.25$.

(3) For the cases of $0 \leqslant K \leqslant 1.0$, the time series of the drag coefficient C_d suggest that the flow around the hill under weak stratification reaches an almost steady condition. On the other hand, the persistent periodical C_d oscillations for the cases of $K = 1.25$ and 1.5 are observed, and for the cases of $K = 1.75$ and 2.0 the C_d oscillations rapidly decay after $t = 200$.

(4) For the cases of $K = 1.25$ and 1.5, the flow unsteadiness associated with the periodical variation of C_d is caused by the "shedding" of the columnar disturbance (eddy) from the hill. A high-C_d state corresponds to the situation where the columnar disturbance (eddy) has just detached from the hill, while a low-C_d state corresponds to the situation where the columnar disturbance (eddy) is just about to detach from the hill.

(5) For the cases of $K = 1.75$ and 2.0, the flow around the hill reaches a steady condition because of the appearance of the columnar disturbance with mode $n = 2$.

Acknowledgements

We would like to thank the referees for their helpful suggestions which have been incorporated in the final manuscript. Thanks are also due to Dr. Ozono of Research Institute of Applied Mechanics of Kyushu University for his variable discussions in numerical simulations.

References

[1] P.G. Baines, Topographic Effects in Stratified Flows, Cambridge University Press, Cambridge, 1994, pp. 224–336.
[2] I.P. Castro, W.H. Snyder, P.G. Baines, Obstacle drag in stratified flow, Proc. Roy. Soc. London A 429 (1990) 119–140.
[3] I.P. Castro, Effects of stratification on separated wakes: part I. Weak static stability, Proc. 3rd IMA Meetings on Stably Stratified flows, Leeds, 1989.
[4] H. Hanazaki, Upstream advancing columnar disturbances in two-dimensional stratified flow of finite depth, Phys. Fluids A 1 (1989) 1976–1987.
[5] H. Hanazaki, Drag coefficient and upstream influence in three-dimensional stratified flow of finite depth, Fluid Dynamics Res. 4 (1989) 317–332.
[6] K.G. Lamb, Numerical simulations of stratified inviscid flow over a smooth obstacle, J. Fluid Mech. 260 (1994) 1–22.
[7] M.F. Paisley, I.P. Castro, N.J. Rockliff, Steady and unsteady computations of strongly stratified flows over a vertical barrier, in: Stably Stratified Flows: Flow and Dispersion over Topography, Clarendon, Oxford University Press, Oxford, 1994, pp. 39–59.
[8] Y. Ohya et al., Stratified flow over a 2-D semicircular cylinder in fluid of finite depth, Proc. 12th Japan Wind Engng Symp., 1992, pp. 13–18 (in Japanese).
[9] T. Uchida et al., A numerical study of stably stratified flows over a two-dimensional hill – Part I. Free-slip condition on the ground, Proc. 9th Japan CFD Symp., 1995, pp. 465–466 (in Japanese).
[10] H. Suito, K. Ishii, Simulation of dynamic stall by multi-directional finite- difference method, AIAA 95-2264, 1995.